Science Signaling
AAAS

www.sciencesignaling.org/cgi/content/full/7/338/ra75/DC1

Supplementary Materials for

Targeting aPKC disables oncogenic signaling by both the EGFR and the proinflammatory cytokine TNFα in glioblastoma

Yael Kusne, Eugenio A. Carrera-Silva, Anthony S. Perry, Elisabeth J. Rushing, Edward K. Mandell, Justin D. Dietrich, Andrea E. Errasti, Daniel Gibbs, Michael E. Berens, Joseph C. Loftus, Christopher Hulme, Weiwei Yang, Zhimin Lu, Kenneth Aldape, Nader Sanai, Carla V. Rothlin,* Sourav Ghosh*

*Corresponding author. E-mail: carla.rothlin@yale.edu (C.V.R.); sourav.ghosh@yale.edu (S.G.)

Published 12 August 2014, *Sci. Signal.* **7**, ra75 (2014)
DOI: 10.1126/scisignal.2005196

The PDF file includes:

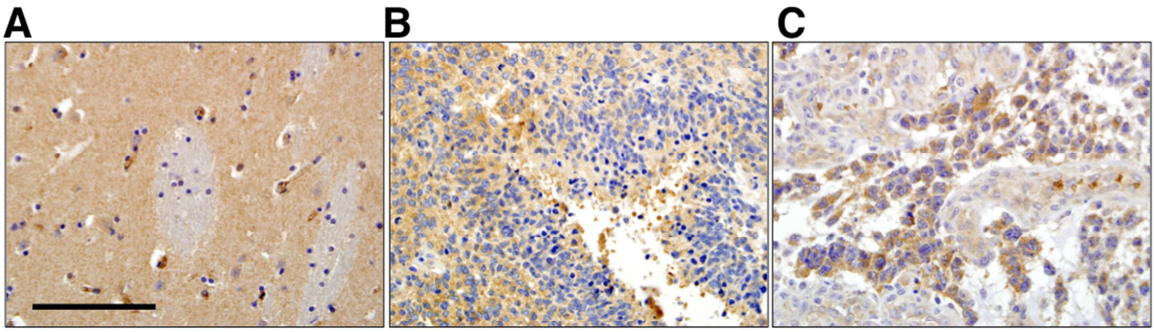

Fig. S1. aPKC immunostaining in nontumor brain and in histologically characteristic regions of glioblastoma. Representative images of aPKC staining in (**A**) normal basal ganglia, (**B**) regions of pseudopalisading necrosis in glioblastoma and (**C**) microvascular proliferation in glioblastoma. Data for (**A**) to (**C**) are representative of more than 50 samples examined. Scale bar: 500 μm

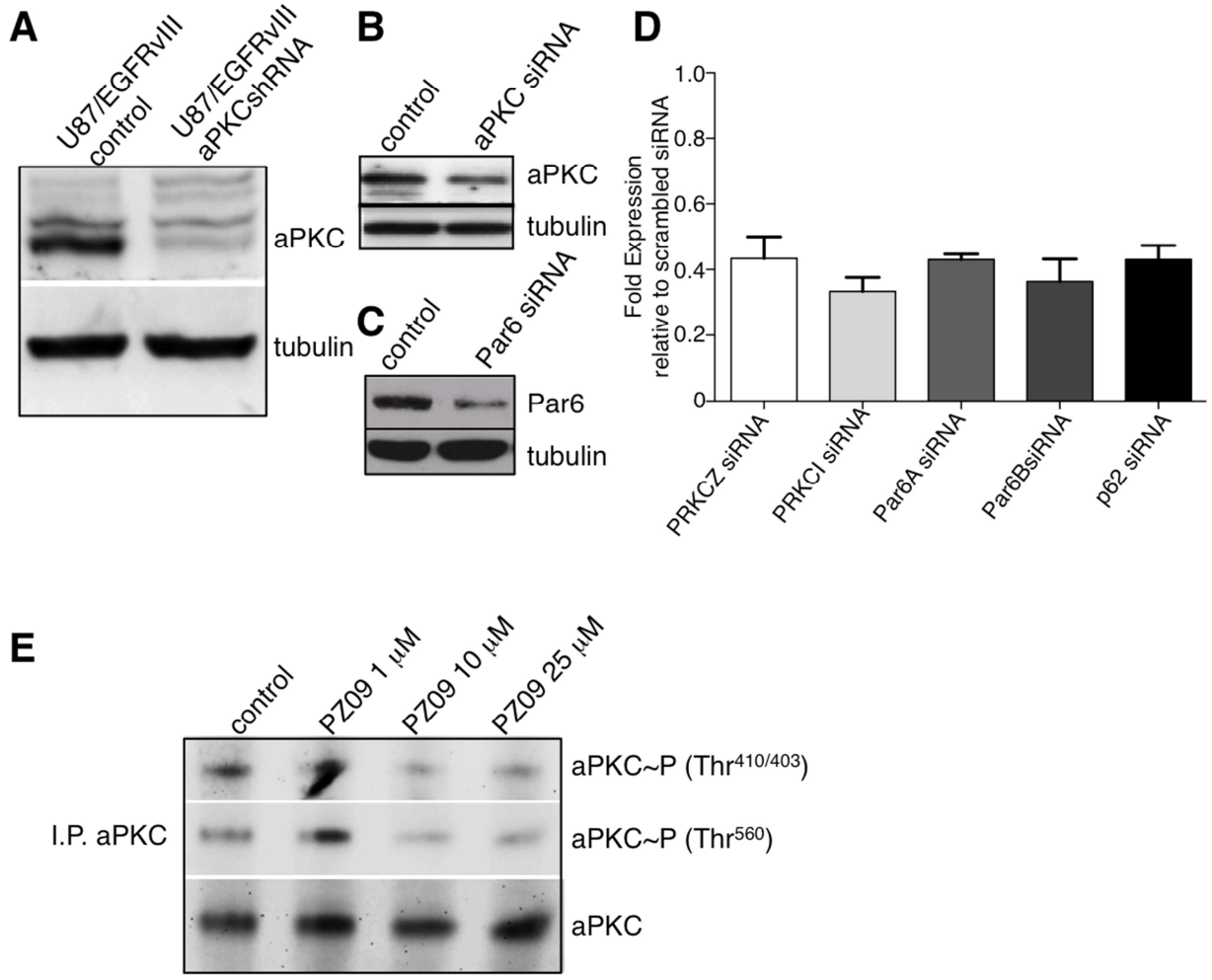

Fig. S2. Validation of aPKC knockdown efficiencies and the inhibitory effect of PZ09. (**A**) aPKC immunoblots of U87/EGFRvIII control cells and U87/EGFRvIII cells expressing aPKC shRNA used for *in vivo* intracranial orthotopic xenograft experiments. (**B**) aPKC immunoblots of U251/EGFR cells transfected with luciferase or aPKC siRNA. (**C**) Par6 immunoblot of U251/EGFR cells transfected with luciferase or Par6 siRNA. (**D**) Knockdown efficiencies in U251/EGFR cells for each indicated gene, normalized to control (luciferase) siRNA, as measured by RT-qPCR. (**E**) Inhibition of aPKC activation in GBM6 with increasing concentrations of PZ09 detected after aPKC immunoprecipitation followed by aPKC phosphoThr$^{410/403}$ or phosphoThr^{560} immunoblotting. Blots were stripped and reprobed with aPKC antibodies. Data for (A) to (E) are presented as representative images or as mean ± SEM of at least 3 independent experiments.

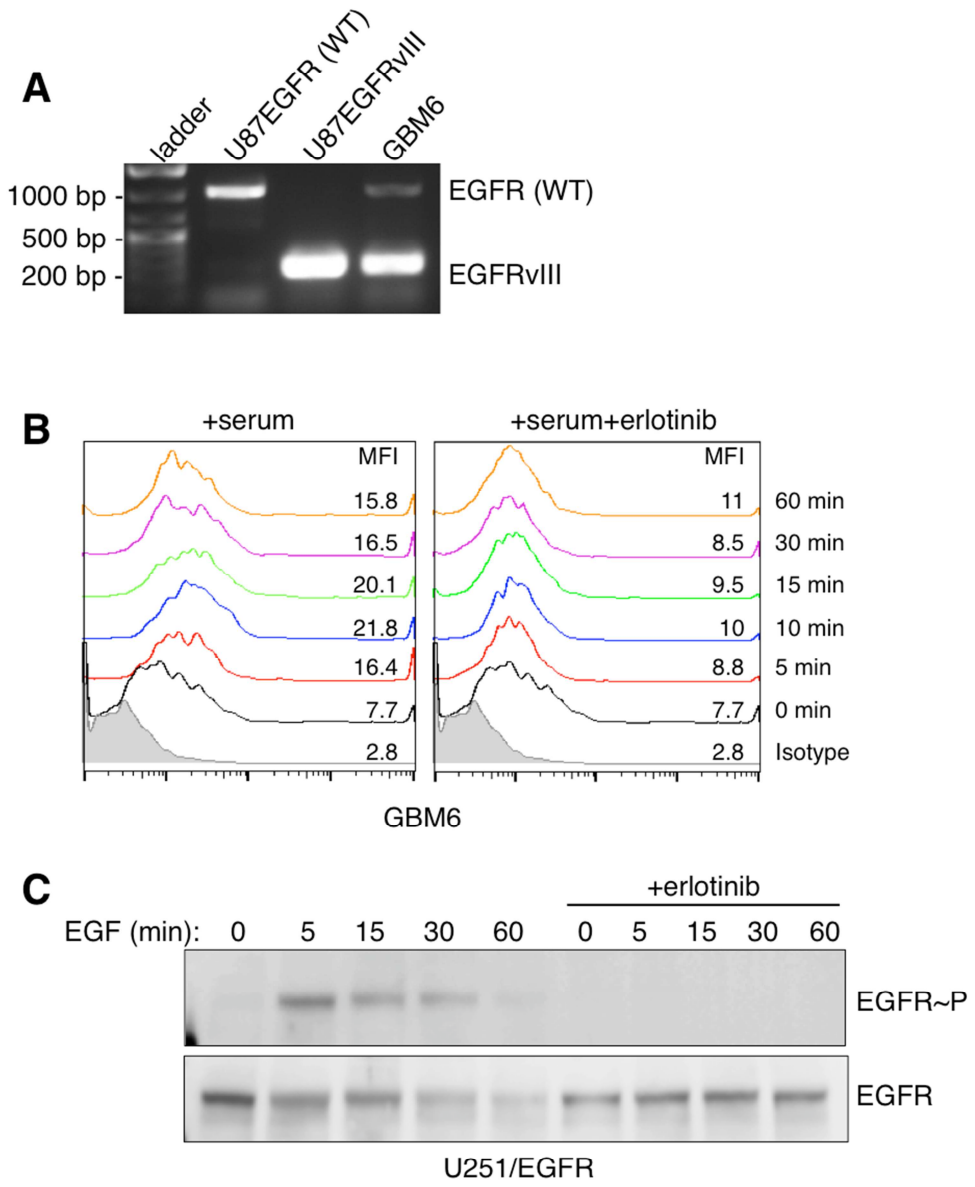

Fig. S3. EGFR isoform abundance in GBM6 and EGFR phosphorylation kinetics in GBM6 and U251/EGFR cells. (**A**) The abundance of EGFR WT and EGFRvIII in GBM6 cells as detected by RT-PCR. U87EGFR (WT) and U87EGFRvIII cells were included as positive controls. (**B**) Representative FACS histograms of EGFR phosphorylation (p-Y^{1086}) kinetics in GBM6 cells. Serum was used to stimulate serum-starved GBM6 cells or serum-starved GBM6 cells pretreated for 30 min with 10 μM erlotinib. (**C**) Representative immunoblots for EGFR phosphorylation (p-Y^{1086}) in serum-starved U251/EGFR cells at various time points as indicated after stimulation with 100 ng EGF alone or 100 ng EGF after 30 min pre-treatment with 10 μM erlotinib. Data for (A) to (C) are representative of at least 3 independent experiments.

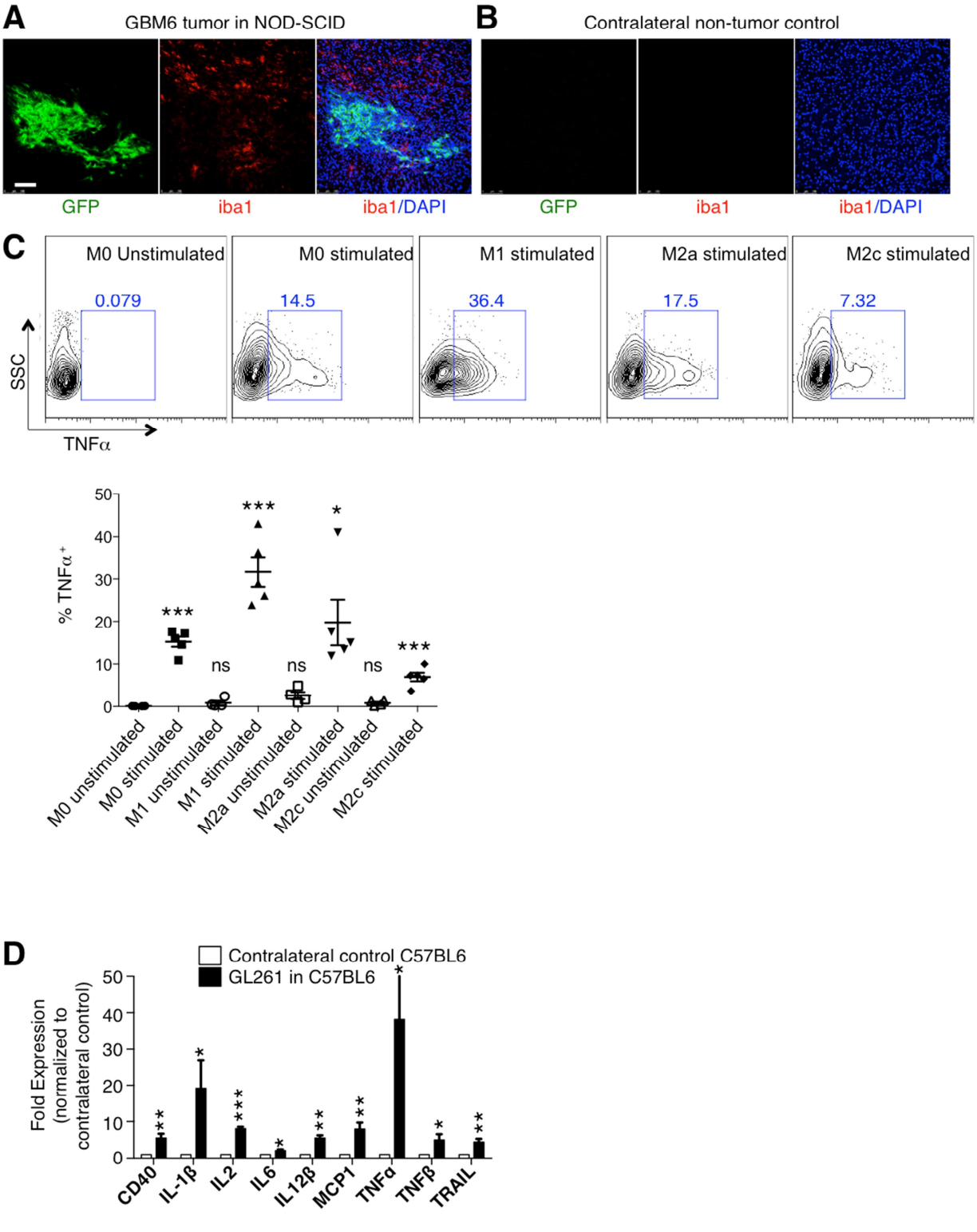
A
GBM6 tumor in NOD-SCID
GFP
iba1
iba1/DAPI
B
Contralateral non-tumor control
GFP
iba1
iba1/DAPI
C
M0 Unstimulated
M0 stimulated
M1 stimulated
M2a stimulated
M2c stimulated
0.079
14.5
36.4
17.5
7.32
SSC
TNFα
% TNFα+
50
40
30
20
10
0
***
ns
ns
*
ns
***
M0 unstimulated
M0 stimulated
M1 unstimulated
M1 stimulated
M2a unstimulated
M2a stimulated
M2c unstimulated
M2c stimulated
D
Contralateral control C57BL6
GL261 in C57BL6
Fold Expression
(normalized to
contralateral control)
50
40
30
20
10
0
CD40
IL-1β
IL2
IL6
IL12β
MCP1
TNFα
TNFβ
TRAIL

Fig. S4. Myeloid cells, TNFα production, and NF-κB activation in mouse models of glioblastoma. (**A** and **B**) Representative images of Iba1 staining of NOD/SCID mouse brain bearing GFP^+ U87vIII/EGFR tumors (B) in comparison to the contralateral, non-tumor bearing side (A). Scale bar: 100 μm. (**C**) Representative FACS analysis (top) and % $TNF\alpha^+$ cells (bottom) in unstimulated and ionomycin- and PMA-stimulated human monocyte-derived macrophages (M0), M1, M2a and M2c. (**D**) Expression of NF-κB target genes in acutely isolated tissue from the side of C57B6 mouse brain bearing GL261 cell-derived tumors in comparison to contralateral, non-tumor bearing brain as detected by RT-qPCR. Data for (A) to (D) are presented as representative images or as mean ± SEM of at least 3 independent experiments.

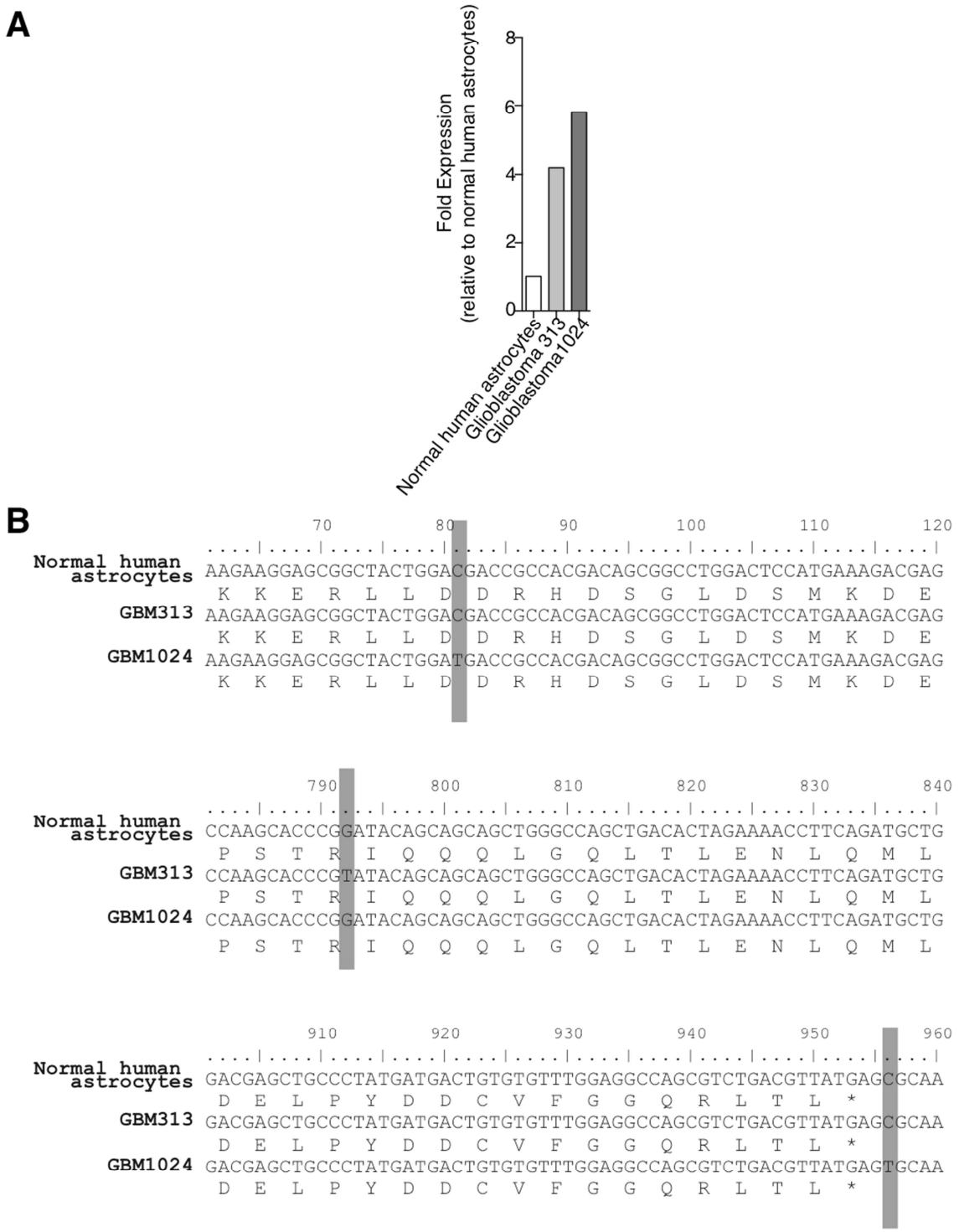

Fig. S5. Expression and sequence of *NFKB1A* in two independent glioblastoma specimens. (**A**) Expression of *NFKB1A* in normal human astrocyte and two independent EGFR+ glioblastoma specimens, as detected by RT-qPCR. mRNA abundance was normalized to normal human astrocytes. (**B**) Sequence from the coding region of IκBα showing three synonymous substitutions. No nonsynonymous mutations were detected.

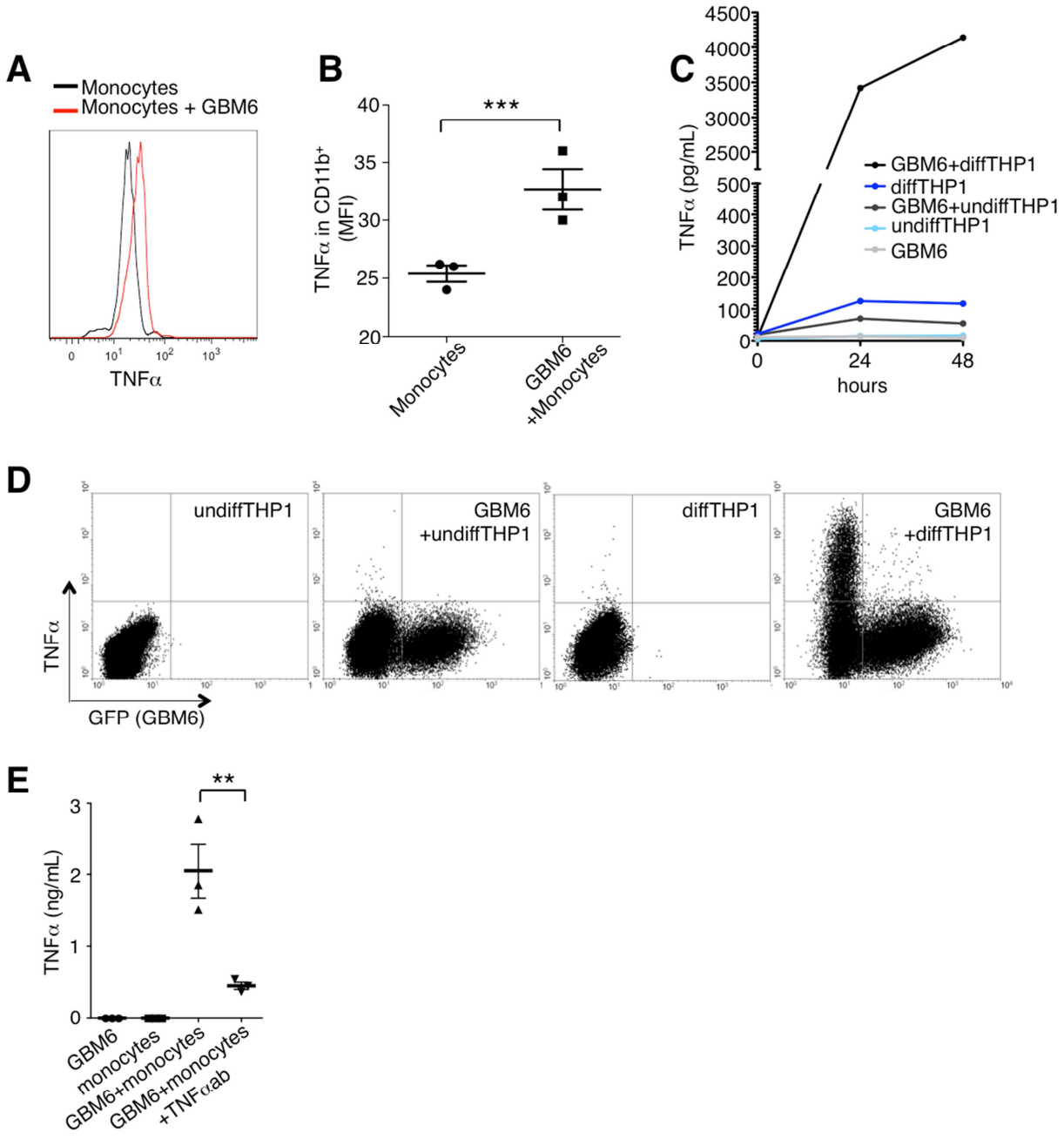

Fig. S6. Myeloid cells produce TNFα when cocultured with glioblastoma cells. (**A**) Representative FACS analysis and (**B**) mean fluorescence intensity (MFI) of TNFα expression in $CD11b^+$ human monocytes upon culture with GBM6 cells. (**C**) TNFα concentration as measured by ELISA in conditioned media from GBM6 cells alone, THP1 cells alone, or indicated cells upon co-culture. Graph shows data from a representative experiment. (**D**) Representative FACS analysis of TNFα from undifferentiated or differentiated THP1 cells upon culture with or without GBM6 cells expressing GFP. (**E**) TNFα concentration as measured by ELISA in conditioned media from GBM6 cells, monocytes, GBM6 cells co-cultured with monocytes in the presence of 100 ng/mL isotype control or TNFα neutralizing antibody. Data for (A) to (E) are presented as representative plots or as mean ± SEM of at least 3 independent experiments. $^{**}p < 0.01$, $^{***}p < 0.001$.

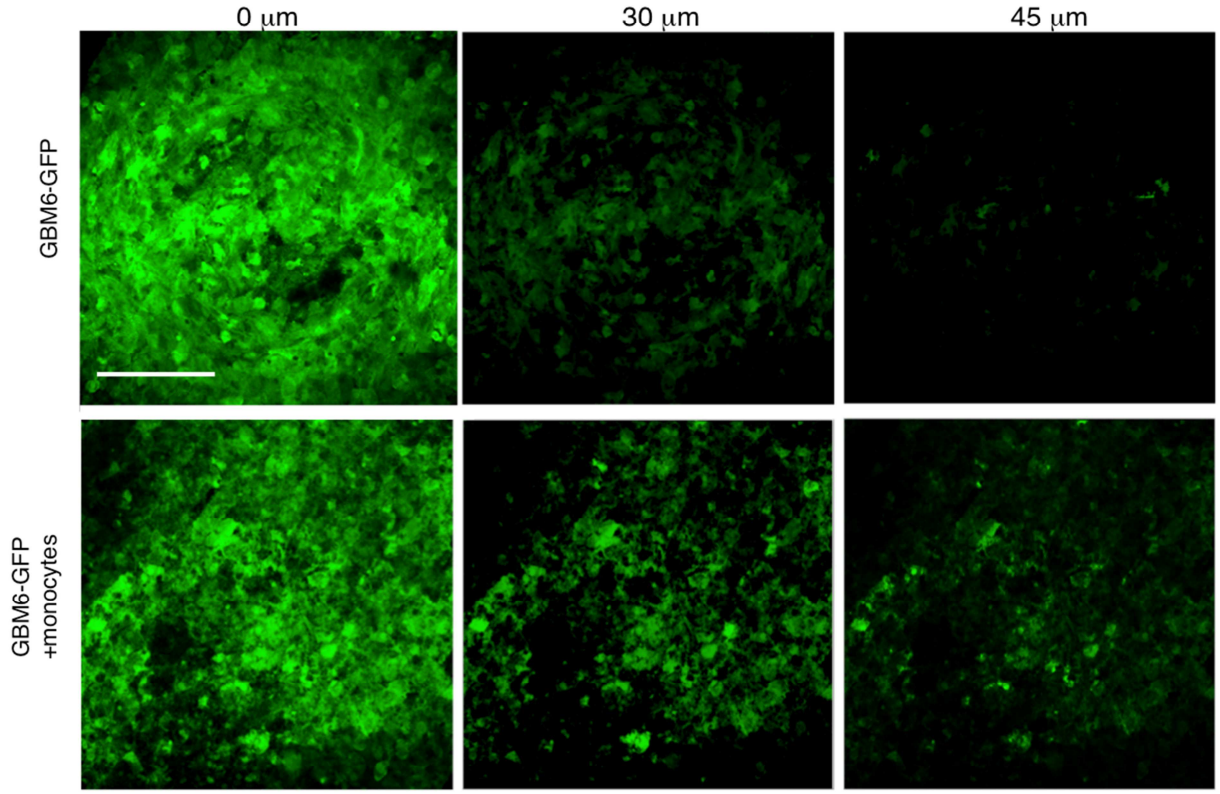

Fig. S7. Coculture with monocytes increases GBM6 cell invasion. Representative images of GFP-labeled GBM6 cells cultured alone or in presence of primary human monocytes at the indicated depth within organotypic cultures of rat brain slice. Data are representative of 3 independent experiments. Scale bar: 100 μm.

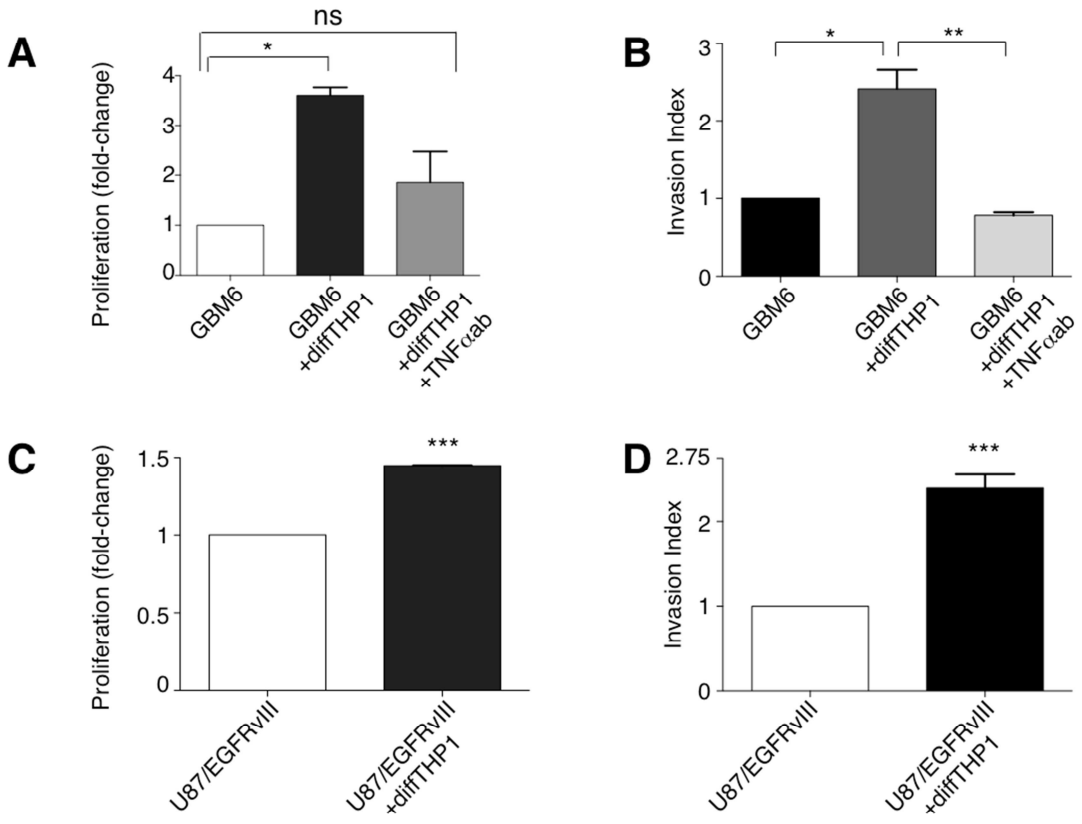

Fig. S8. Human myeloid cell–derived TNFα contributes to increased proliferation and invasion of GBM6 cells. (**A**) Proliferation of GBM6 cells upon culture with differentiated THP1 cells in the presence of isotype control or neutralizing monoclonal anti-TNFα antibody and normalized to the proliferation of GBM6 cells alone. (**B**) Invasion indices of GBM6 cells upon culture with differentiated THP1 cells in the presence of isotype control or neutralizing monoclonal anti-TNFα antibody and normalized to the invasion index of GBM6 cells cultured alone. (**C**) Proliferation of U87/EGFRvIII cells upon culture with differentiated THP1 cells and normalized to control. (**D**) Invasion indices of U87/EGFRvIII cells upon culture with differentiated THP1 cells and normalized to control. Data for (A) to (D) are presented as mean ± SEM of at least 3 independent experiments. *$p < 0.05$, **$p < 0.01$, ***$p < 0.001$, ns is non significant.

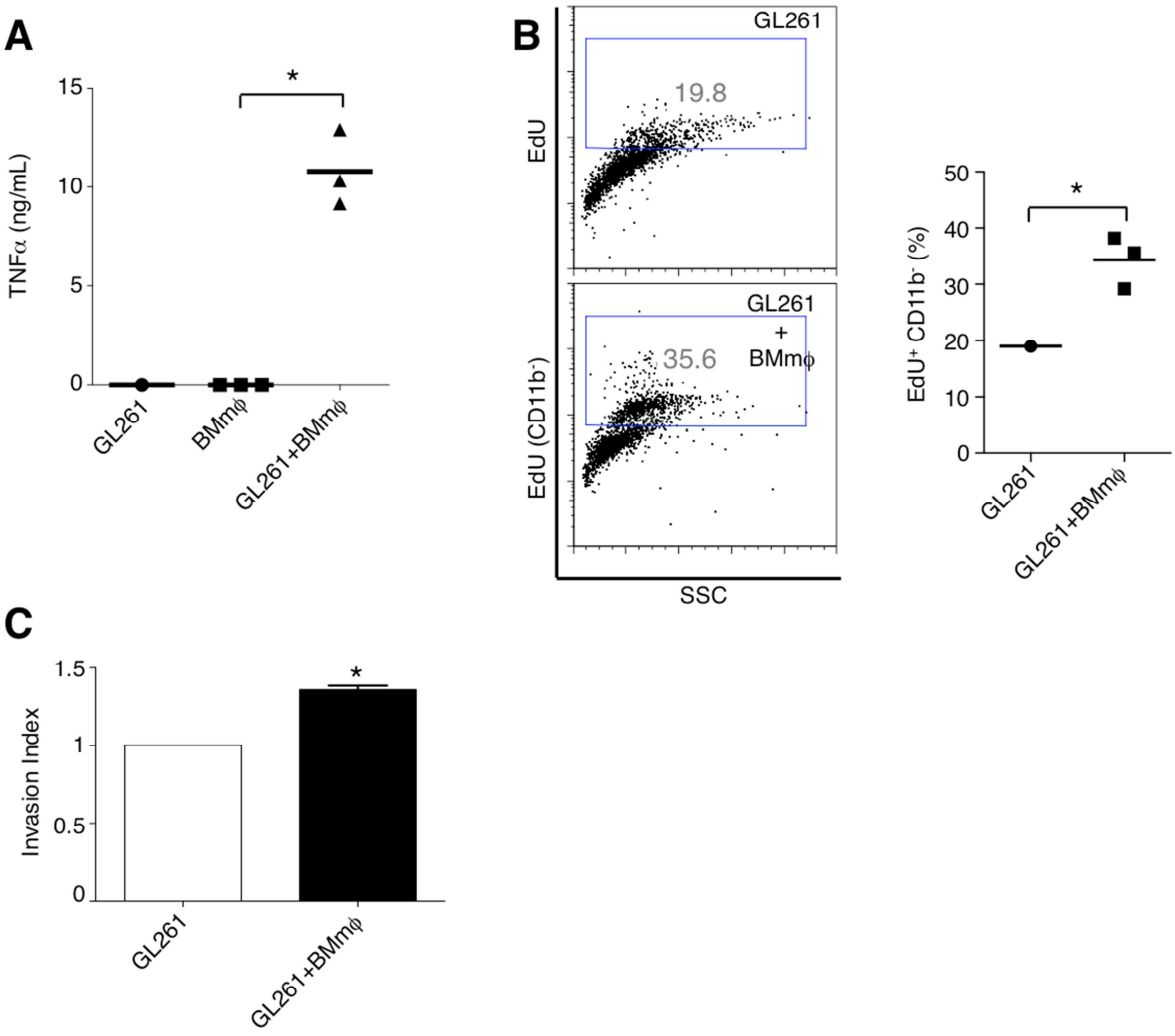

Fig. S9. Murine myeloid cell–derived TNFα contributes to increased glioblastoma proliferation and invasion. (**A**) TNFα concentration as measured by ELISA in culture media of GL261 cells alone, primary mouse macrophages alone, or GL261 cells upon culture with primary mouse macrophages. (**B**) Representative FACS analysis (left panel) and percentage (%, right panel) of EdU incorporation in GL261 cells upon culture with primary mouse macrophages. (**C**) Invasion index of GL261 cells upon culture with primary mouse macrophages. *$p < 0.05$.

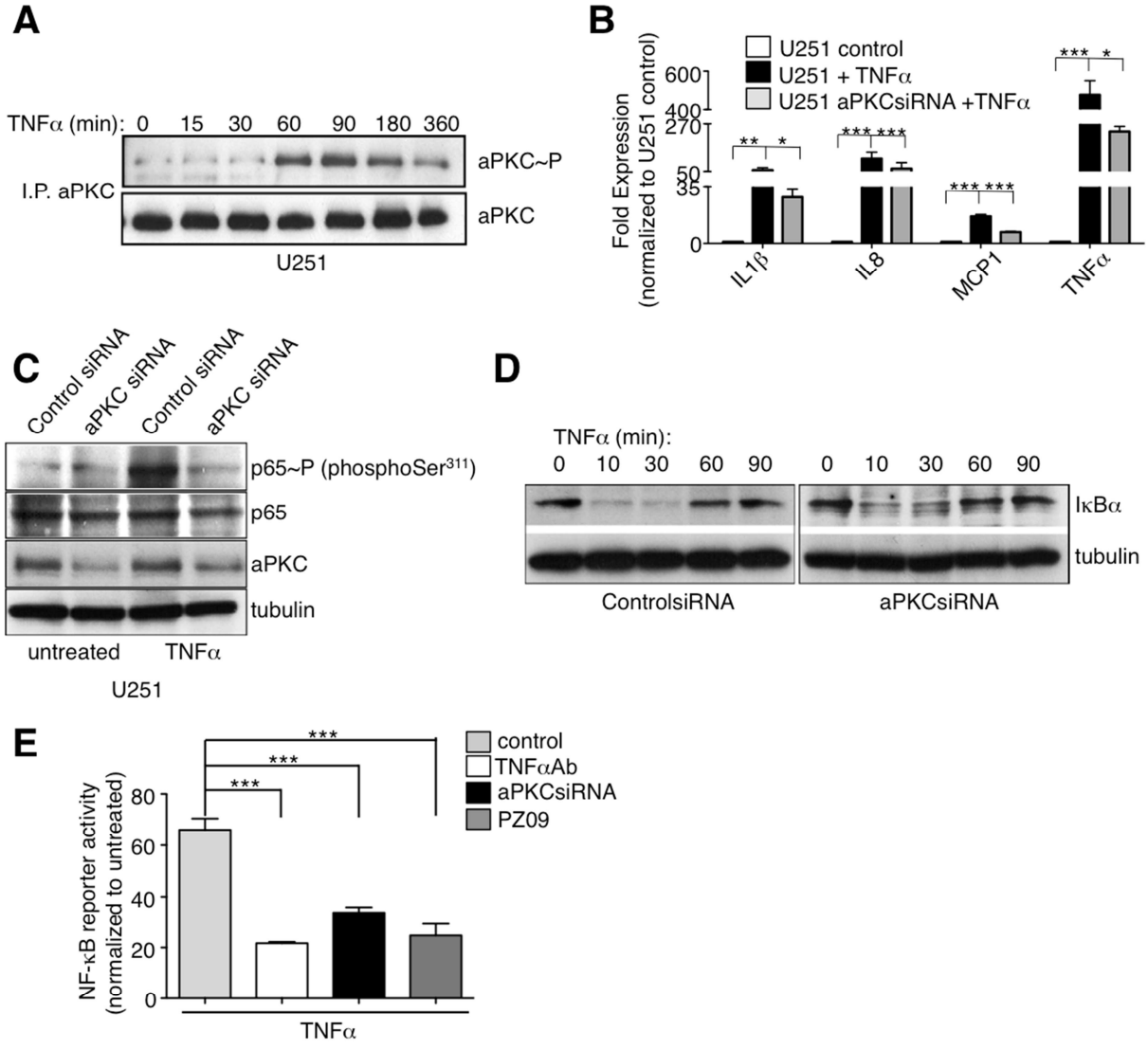

Fig. S10. TNFα-induced NF-κB signaling in U251/EGFR cells depends on aPKC. (A) Activation of aPKC in U251/EGFR cells treated with TNFα for the indicated times. (B) Expression of NF-κB target genes in untreated U251/EGFR cells or those transfected with aPKC siRNA after TNFα treatment, as detected by RT-qPCR. mRNA abundance was normalized to U251/EGFR control cells. (C) Phosphorylation of Ser^{311} in p65 in U251/EGFR cells or those cells transfected with aPKC siRNA after TNFα treatment. β-tubulin was used as a loading control and the aPKC immunoblot shows the extent of aPKC silencing. (D) Immunoblot of IκBα in control U251/EGFR (controlsiRNA) cells or U251/EGFR cells in which aPKC expression has been silenced (aPKCsiRNA) after 10 ng/mL TNFα treatment for the indicated times. β-tubulin blotting was used for loading control. (E) TNFα-stimulated NF-κB fluorescent reporter activity in untreated U251/EGFR cells or cells incubated with the anti-human TNFα antibody, transfected with aPKC siRNA or treated with PZ09. Data for (A) to (E) are presented as representative or mean ± SEM of at least 3 independent experiments. *$p < 0.05$, **$p < 0.01$, ***$p < 0.001$.

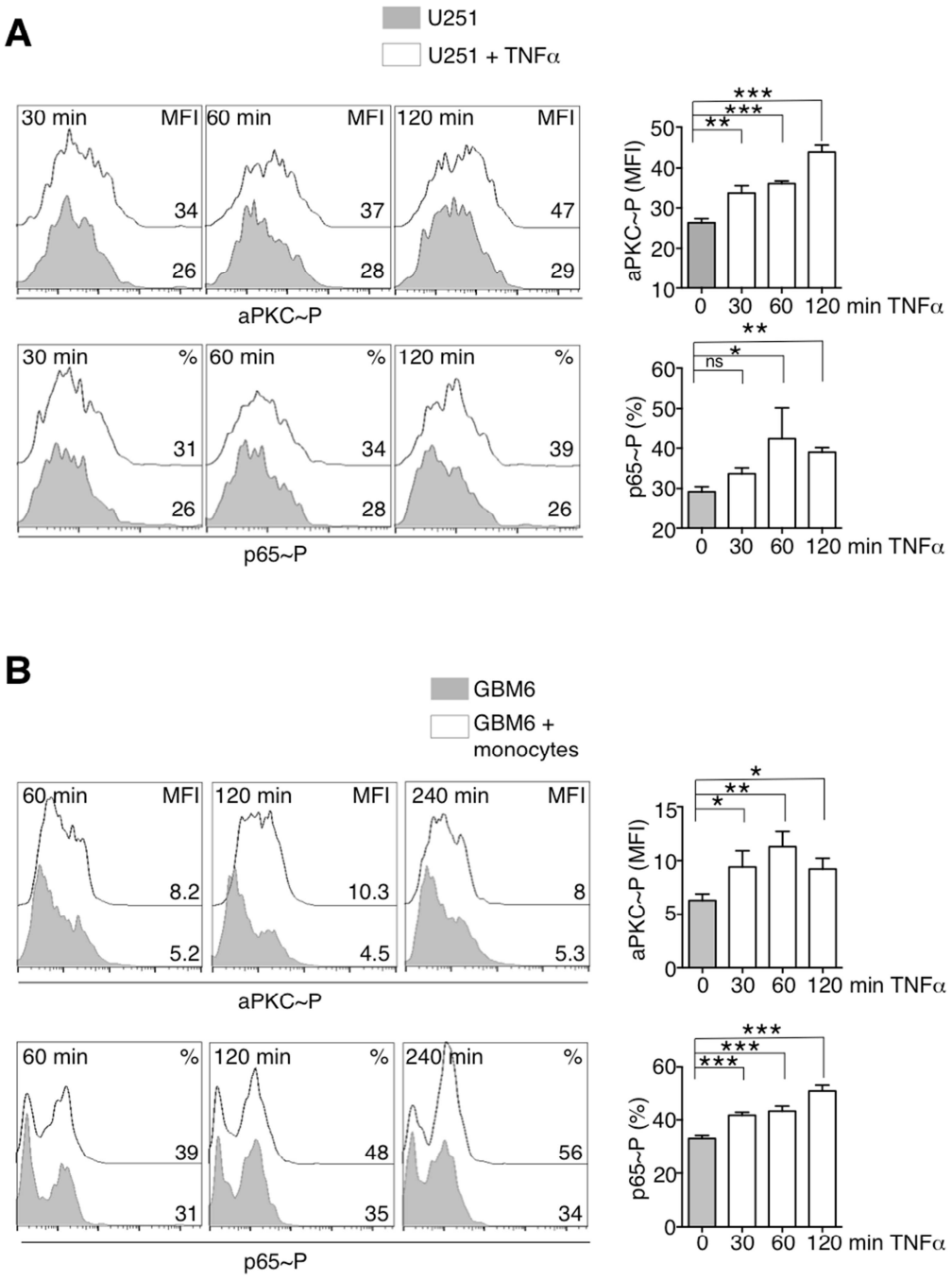

Fig. S11. Phosphorylation of aPKC precedes phosphorylation of p65. (**A**) Representative FACS histograms of aPKC Thr^{560} (left) and NF-κB p65 Ser^{536} (right) phosphorylation at the indicated times in U251 cells alone and upon stimulation with 10 ng/mL TNFα. (**B**) Representative FACS histograms of the phosphorylation of aPKC at Thr^{560} (left) and NF-κB p65 at Ser^{536} (right) in GBM6 cells alone and upon co-culture with monocytes at the indicated time points. Data are presented as representative histograms of at least 3 independent experiments.

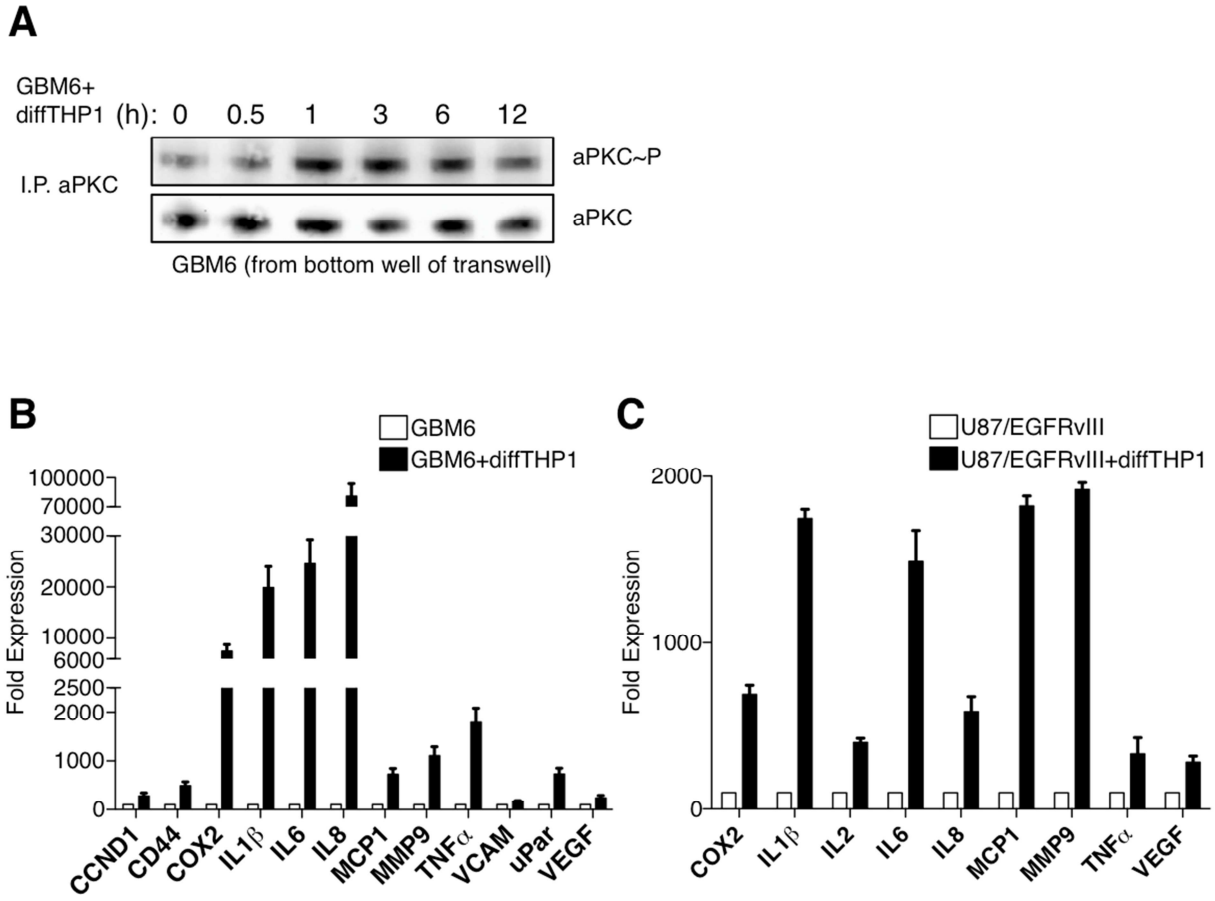

Fig. S12. Activation of aPKC and induction of NF-κB–dependent genes in glioblastoma cells upon coculture with myeloid cells. (**A**) GBM6 cells were grown on the bottom compartment of a transwell culture system and GBM6 cells together with differentiated THP1 cells were co-cultured in the top compartment for the indicated times. Active aPKC in GBM6 from the bottom compartment at the indicated times was detected after aPKC immunoprecipitation followed by aPKC phosphoThr$^{410/403}$ immunoblotting. (**B**) Expression of the indicated genes in GBM6 cells and (**C**) U87/EGFRvIII cells upon culture with differentiated THP1 cells for 24 h as measured by RT-qPCR. GBM6 cells or U87/EGFRvIII cells were grown on the bottom compartment of a transwell culture system and GBM6 or U87/EGFRvIII cells together with differentiated THP1 cells were co-cultured on the top for the indicated times. Data for (A) to (C) are presented as representative images or as mean ± SEM of at least 3 independent experiments.

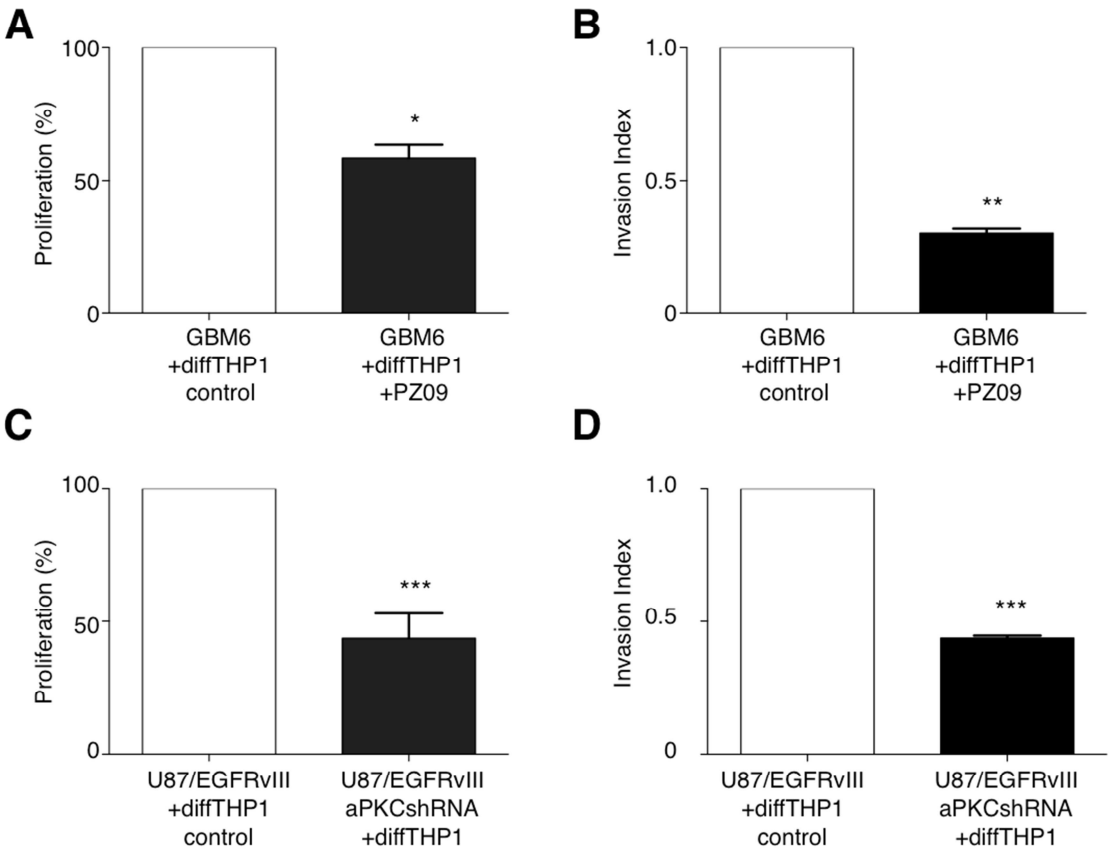

Fig. S13. Myeloid cell–mediated induction of proliferation and invasion of glioblastoma cells depends on aPKC. (**A**) Proliferation (percentage) of GBM6 cells upon culture with THP1 cells in the presence or absence of 10 μM PZ09. (**B**) Invasion indices of GBM6 cells upon culture with THP1 cells in the presence or absence of 10 μM PZ09. (**C**) Proliferation (percentage) of U87/EGFRvIII cells or cells with aPKC knockdown upon culture with differentiated THP1 cells. (**D**) Invasion indices of control U87/EGFRvIII cells or cells with aPKC knockdown upon culture with differentiated THP1 cells. Data for (A) to (D) are presented as mean ± SEM of at least 3 independent experiments. *$p < 0.05$, **$p < 0.01$, ***$p < 0.001$.

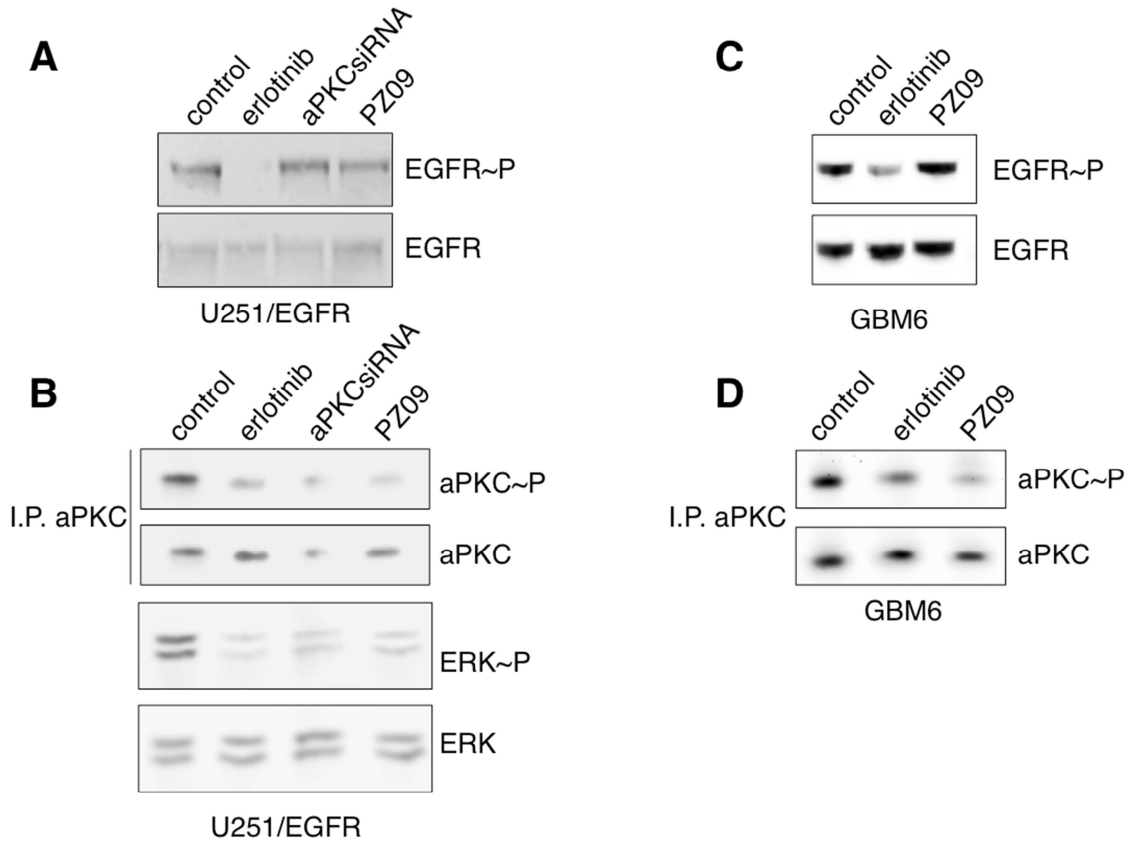

Fig. S14. aPKC inhibition does not suppress the phosphorylation of EGFR. (**A**) EGFR phosphorylation in U251/EGFR cells alone (control), upon incubation with 10 μM concentration of erlotinib, in U251/EGFR cells in which aPKC expression has been silenced (aPKCsiRNA) or upon incubation with 10 μM of PZ09. (**B**) Immunoblots of aPKC phosphorylation and total aPKC after immunoprecipitation (I.P.) in U251/EGFR cells treated as in A (top panels). Immunoblots of ERK phosphorylation and total ERK in U251/EGFR cells treated as in A (bottom panels). (**C**) Immunoblots of EGFR phosphorylation in GBM6 cells alone (control), upon incubation with 10 μM of erlotinib or 10 μM of PZ09. (**D**) Immunoblots of aPKC phosphorylation and total aPKC after immunoprecipitation (I.P.) in GBM6 cells treated as in C. The blots in (A) to (D) are representative of at least 3 independent experiments.

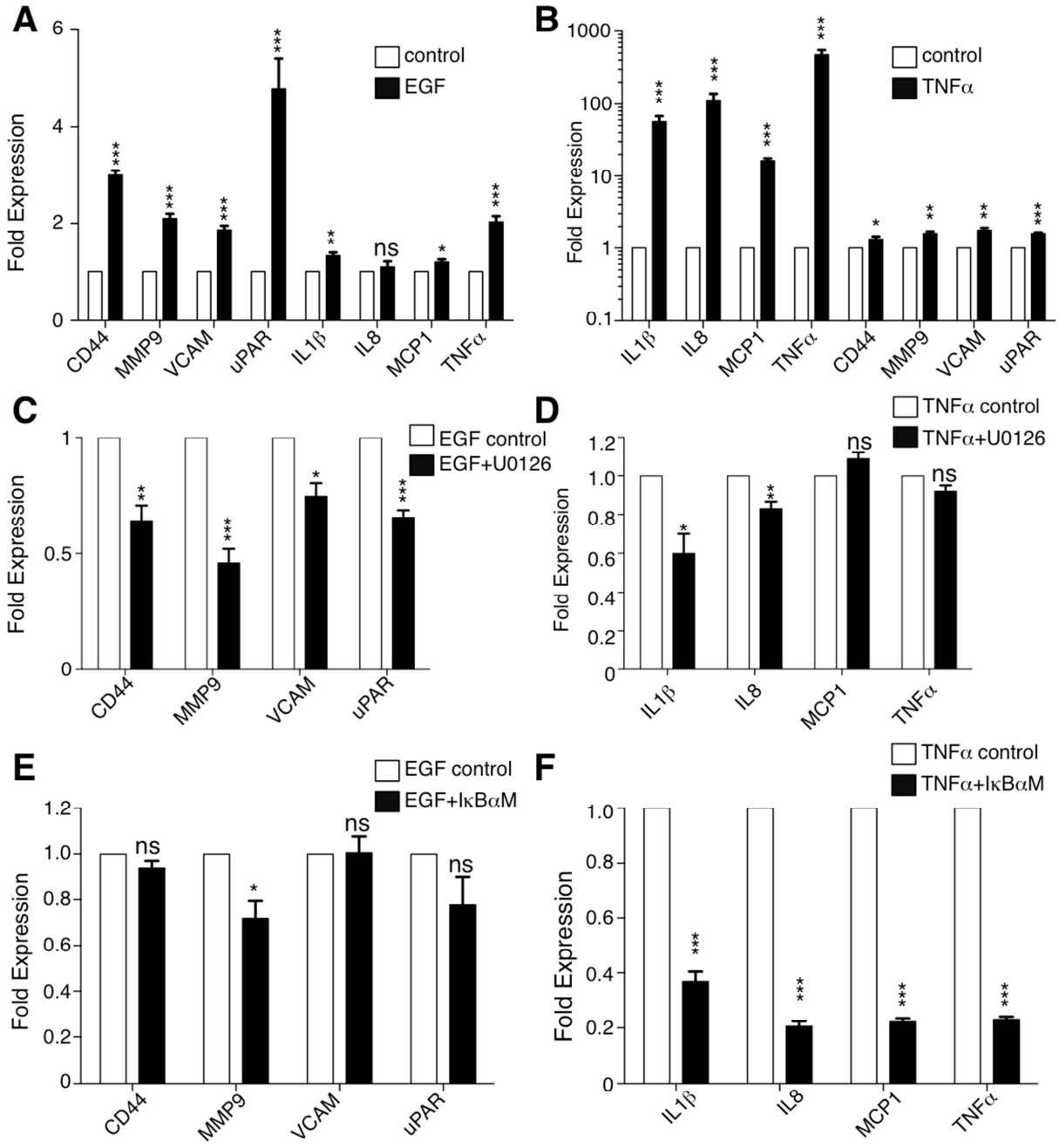

Fig. S15. Induction of distinct sets of genes by EGF and TNFα signaling in glioblastoma cells. (**A**) Expression of the indicated genes in U251/EGFR cells treated with 100 ng/mL EGF for 6 h or (**B**) 10 ng/mL TNFα for 1 h, as detected by RT-qPCR. (**C**) Expression of the indicated genes in U251/EGFR cells treated with 100 ng/mL EGF for 6 h or (**D**) 10 ng/mL TNFα for 1 h with or without 10 μM U0126, as detected by RT-qPCR. (**E**) Expression of the indicated genes in U251/EGFR cells transduced with IκBαM-expressing virus and treated with 100 ng/mL EGF for 6 h or (**F**) 10 ng/mL TNFa for 1 h. Data for (A) to (F) are presented as mean ± SEM of at least 3 independent experiments. *p < 0.05, **p < 0.01, ***p < 0.001, ns is non significant.

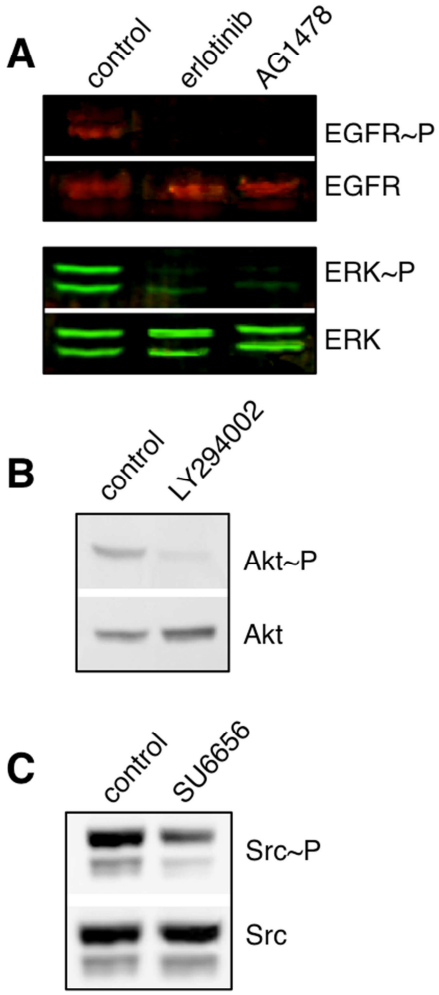

Fig. S16. Validation of EGFR, AKT, and Src inhibition in U87/EGFRvIII cells. (**A**) Immunoblots of phosphorylated and total EGFR and phosphorylated and total ERK in cell lysates from U87/EGFRvIII control cells or in cells incubated with 10 μM of erlotinib or 10 μM of AG1478 for 30 min. (**B**) Immunoblots of phosphorylated and total AKT in cell lysates from U87/EGFRvIII control cells or in cells incubated with 20 μM of LY294002 for 30 min. (**C**) Immunoblots of phosphorylated and total Src in cell lysates from U87/EGFRvIII control cells or in cells incubated with 10 μM of SU6656 for 30 min. The blots in (A) to (D) are representative of at least 3 independent experiments.

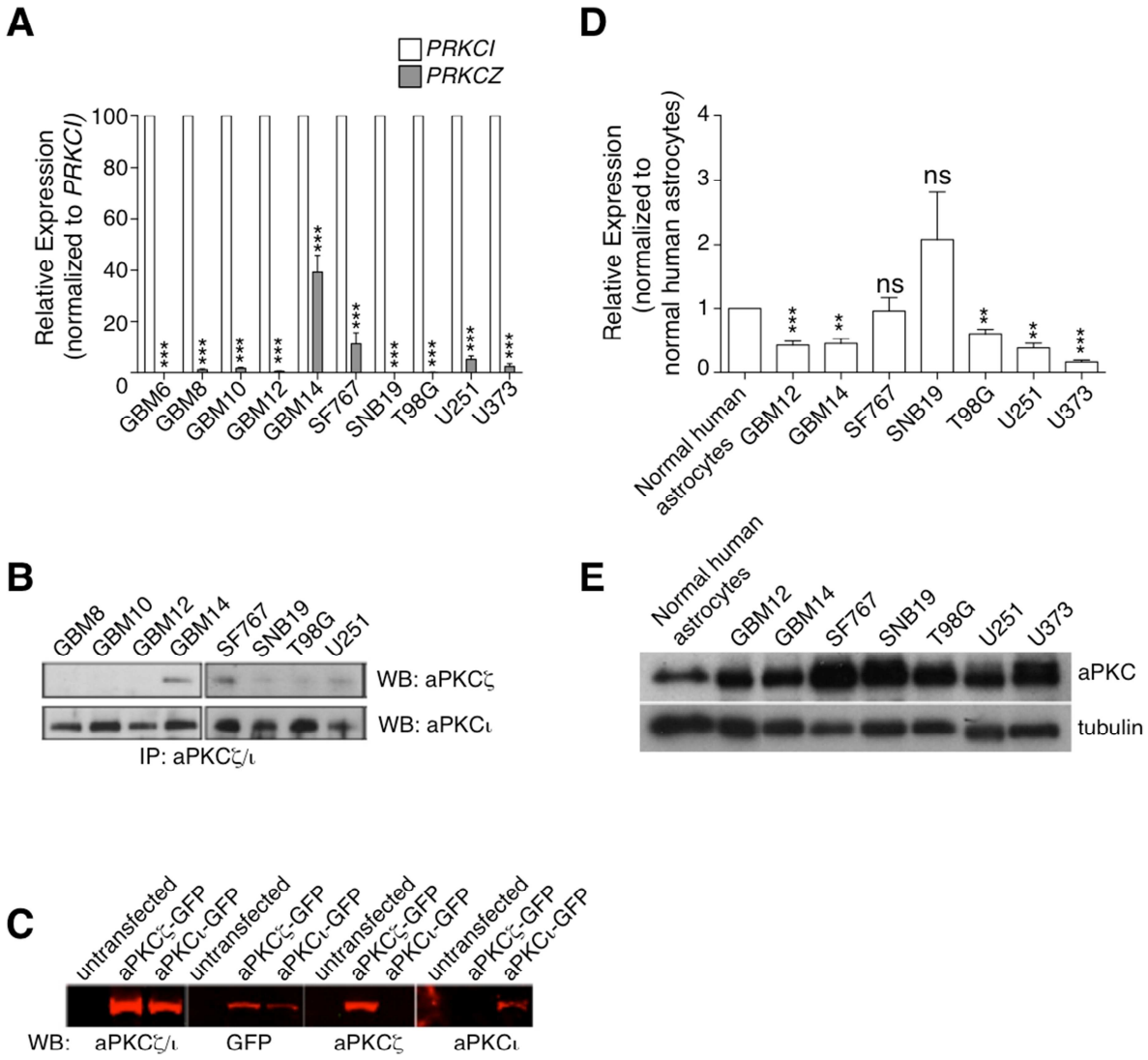

Fig. S17. *PRKCI* is the predominant aPKC isoform that shows increased abundance in glioblastoma. (**A**) Relative expression of aPKCi *(PRKCI)* and aPKCz (*PRKCZ)* in patient-derived xenografts (GBM8, GBM10, GBM12, and GBM14) and glioblastoma cell lines (SF767, SNB19, T98G, U251, U373) as detected by RT-qPCR using isoform specific primers. Relative abundance of the isoforms normalized to *PRKCI* is shown. (**B**) Abundance of aPKCi and aPKCz as detected by immunoblotting using isoform specific antibodies. Total aPKC was immunoprecipitated and probed with isoform specific antibodies. (**C**) Validation of isoform specific antibodies on HEK293 cells expressing aPKC-GFP fusion protein as detected by Western blotting using total aPKC antibody and isoform specific aPKC antibodies. (**D**) Relative abundance of aPKCi in the indicated cells as detected by RT-qPCR using isoform-specific primers and normalized to human astrocytes. (**E**) Abundance of total aPKC as detected by immunoblotting in the indicated cells. Tubulin is shown as loading control.

Table S1. List of primers.

Primer (RT-qPCR)	Forward	Reverse
PRKCI	CACTCCAGATGACGATGACATTG	TGCAGACATCAAAAGAGGATTGA
PRKCZ	CGCTCCCCGTTCGACAT	CCAGGATCAGGAAAAGGT
ACTB	TCCCTGGAGAAGAGCTACG	GTAGTTTCGTGGATGCCACA
CD44	CCCATCCCAGACGAAGACAG	ACCATGAAAACCAATCCCAGG
COX2	TTAATGAGTACCGCAAACGC	ACCAGAAGGGCAGGATACAG
GAPDH	TGCACCACCAACTGCTTAGC	GGCATGGACTGTGGTCATGAG
IL1β	TTCTGCTTGAGAGGTGCTGA	CTGTCCTGCGTGTTGAAAGA
IL6	TGAACTCCTTCTCCACAAGCG	TCTGAAGAGGTGAGTGGCTGTC
IL8	TTTTGCCAAGGAGTGCTAAAG	AACCCTCTGCACCCAGTTTTC
MCP1	GCTCGCTCAGCCAGATGCA	GGACACTTACTGCTGGTGATT
MMP9	CATTTCGACGATGACGAGTTG	CGGGTGTAGAGTCTCTCGC
PARD6A	AGCATCGTCGAGGTGAAGAG	GTATAGCCAAGTAGCACGTCC
PARD6B	GTTGACGTTTTGGTAGGCTATGC	AGTGGATTGGCCGTTGAAACA
P62/SQSTM1	AAGCCGGGTGGGAATGTTG	CCTGAACAGTTATCCGACTCCAT
TNFα	ATGAGCACTGAAAGCATGATC	GAGGGCTGATTAGAGAGAGGT
PLAUR	ACCCATGGTCTTCCATTTGA	GTTGCACCAGTGAATGTTGG
VCAM	TCCACGCTGACCCTGAGCCC	GCTCCCATTCACGAGGCCACC
EGFRvIII-1	GAGCTCTTCGGGGAGCAG	GTGATCTGTCACCACATAATTACCTTTCT
EGFRvIII-2	GGCTCTGGAGGAAAAGAAAGGTAAT	TCCTCCATCTCATAGCTGTCG
EGFR total	TTGCCGCAAAGTGTGTAACG	GTCACCCCTAAATGCCACCG
Primer (sequencing)		
NFKBIA-1	CTCCGAGACTTTCGAGGAAATAC	GCCATTGTAGTTGGTAGCCTTCA
NFKBIA-2	GCGCCCCAGCGAGGAAGCA	CAATAAATATAAAATGTGGTCCTTCC
Primer (RT-PCR)		
EGFR	CTTCGGGGAGCAGCGATGCGAC	ACCAATACCTATTCCGTTACAC

Table S2. List of siRNA and shRNA sequences.

siRNA	Source	siRNA ID	Sequence
Stealth siRNA *Prkcz* D1	Invitrogen	VHS41530	5'-GCUGGUGCAUGAUGACGAGGAUAUU-3' 5'-AAUAUCCUCGUCAUCAUGCACCAGC-3'
Stealth siRNA *Prkcz* D2	Invitrogen	VHS41533	5'-GGGUACAGACAGAGAAGCACGUGUU-3' 5'-AACACGUGCUUCUCUGUCUGUACCC-3'
Stealth siRNA *Pard6A*	Invitrogen	HSS147208	5'-AGGUCUUCCCGGCUACUUCAAUGCC-3' 5'-GGCAUUGAAGUAGCCGGGAAGACCU-3'
Stealth siRNA *Pard6B*	Invitrogen	HSS150023	5'-AUCAUUAACAGCUAAUAGUCCUGUA-3' 5'-UACAGGACUAUUAGCUGUUAAUGAU-3'
Stealth siRNA *p62/SQSTM1*	Invitrogen	HSS113116	5'-AGAAGUGGACCCGUCUACAGGUGAA-3' 5'-UUCACCUGUAGACGGGUCCACUUCU-3'
Stealth siRNA *p62/SQSTM1*	Invitrogen	HSS113117	5'-CAGGCUCCUGCAGACCAAGAACUAU-3' 5'-AUAGUUCUUGGUCUGCAGGAGCCUG-3'
GIPZ Human *Prkcz* shRNA	Open Biosystems	V3LHS_635000	5'-ACAGCTTCCTCCATCTTCT-3' sense 5'-AGAAGATGGAGGAAGCTGT'3' antisense